

## Chapter 2

# Eta-nucleon and Eta-prime-nucleon Coupling constants in QCD and the role of gluons

The complicated mass spectrum of light pseudoscalar mesons, especially, the large mass of  $\eta'$  (958 MeV) meson is believed to be the consequence of the explicit breaking of  $SU(3)_f$  symmetry and breaking of axial  $U(1)$  symmetry at the quantum level [42]. Gluonic degrees of freedom play an important role in the flavor-singlet channel through QCD axial anomaly. Since  $\eta$  and  $\eta'$  both contain singlet component due to mixing, the glue affects both. The gluon impacts the masses of these mesons as well as the interactions of these mesons with other particles. There prevail dramatic differences between these two mesons in reality. Large difference in their masses despite having similar quark content,  $\eta'$ 's strong affinity towards the glue, the deviation of branching ratios of  $B, D_s \rightarrow \eta, \eta'$  from that predicted by models [43], decay of baryonic resonances  $N(1535)$  and  $N(1650)$  via emission of  $\eta$  but not via emission of  $\eta'$  [44, 45] make these mesons differ largely from each other and the interaction of these mesons with other particles also differ significantly. The anomalously large mass of  $\eta'$  which makes it an unsuitable candidate for being a Goldstone boson of spontaneously broken symmetry, indicate that  $\eta'$  is essentially a mixture of both light quarkonium and gluonium and this glue content may have an impact on  $\eta'$  interaction with nucleons.

Kroll and collaborators have concluded quite large, radiatively generated two gluon Fock components in  $\eta'$  wave function [46]. In [47], it has been contended that at low energies ( $Q^2 \approx 2\text{GeV}^2$ ) only about 20% of the momentum of  $\eta$  and  $\eta'$  mesons is carried by gluons in the chiral limit, though at very high energies,  $\sim M_z^2$ , this fraction evolves to 50%. In the case of nucleons, roughly 50% of the momentum is carried by gluons at moderately high energies. This conclusion on momentum fraction carried by gluons is drawn from results on valance quark distribution functions of the hadron following conventional logic. A claim of a significant glue content of  $\eta'$  by KLOE collaboration [48] is based on the fitting measurements on  $\phi \rightarrow \eta'\gamma, \eta\gamma$  together with several radiative decays, such as  $V \rightarrow P\gamma$  and  $P \rightarrow V\gamma$  involving  $\eta'$ ,  $\eta$  mesons. This is in conflict with the analysis of radiative decays  $V \rightarrow P\gamma$  and  $P \rightarrow V\gamma$  by Escribano and Nadal [49], and Thomas [50], who found no evidence for gluonic contribution in  $\eta$  or  $\eta'$ .

The range of the glue induced  $\eta'$ -nucleon interaction, determined by two-gluon effective potential, is found to be of the order of 0.3 fm. The reaction  $pp \rightarrow pp\eta'$ , occurs at distances  $\sim 0.2\text{fm}$ , via which threshold production of  $\eta'$  occurs. At these distances, the quark-gluon degrees of freedom play a significant role in the production dynamics of these mesons [51, 52]. Thus, the gluon induced production mechanism is important as the singlet component of  $\eta$  and  $\eta'$  couple to glue.

Harland-Lang et al. [53] have considered the central exclusive production of  $\eta', \eta$  meson pairs in  $pp(\bar{p})$  collision in the perturbative regime. They show on phenomenological ground that the cross-sections for the production of  $\eta, \eta'$  meson pairs in such processes are strongly sensitive to the size of the gluon content of these mesons. Bass and Moskal [54] have emphasized the fact that the magnitude of the scattering lengths  $a_{\eta N}$  and  $a_{\eta' N}$  are much greater than  $a_{\pi N}$ . They have further pointed out that the search for  $\eta$  and  $\eta'$  mesic nuclei will help understand the dynamics of axial U(1) symmetry breaking in low-energy QCD. The binding energies and in medium masses of the  $\eta$  and  $\eta'$  are sensitive to the flavor singlet component in the mesons

and hence to non-perturbative glue. Experiments at COSY [55], ELSA, GSI/FAIR [56] have been set up to look for bound states of these mesons in nuclei. Gluons in the proton play an essential role in understanding its internal spin structure [57, 58]. Thus, the knowledge of meson-nucleon interaction is important both for nuclear and particle physics.

Due to short life-time of flavor neutral pseudoscalar mesons, experiments with meson beams or targets are difficult and not feasible. Therefore, the meson-nucleon interaction can be studied only via its influence on the cross-sections of the reactions during which they are produced. For  $\eta$  and  $\eta'$ , quantitative information about the interaction can be inferred from the shape of the excitation functions (plot of cross-section versus energy) for the  $pp \rightarrow pp\eta$  and  $pp \rightarrow pp\eta'$  reactions as well as from a comparison of those to the  $pp \rightarrow pp\pi^0$  reaction.

A reliable determination of the coupling constants  $g_{\eta NN}$  and  $g_{\eta' NN}$  would shed considerable light on the axial  $U(1)$  dynamics of QCD [59, 60]. Also,  $g_{\eta NN}$  and  $g_{\eta' NN}$  have essential roles in construction of realistic NN potential [61, 62], in estimates of electric dipole moment of the neutron [63] and in analyses of photoproduction of these mesons [64–66] and scattering involving nucleons and these mesons.

## 2.1 A glimpse on studies of $\eta NN$ , $\eta' NN$ coupling constants

The pion-nucleon coupling constant has been studied widely and the value of  $g_{\pi NN} \simeq 13$  is known with reasonable precision. The Goldberger-Treiman relation (GT relation) for pion reads [67],

$$f_\pi g_{\pi NN} = 2m_N G^{(3)}. \quad (2.1)$$

Where,  $f_\pi$  is the pion-decay constant,  $m_N$  is the mass of the nucleon, and  $G^{(3)}$  is renormalized axial vector coupling constant defined as,

$$\langle N(p, s) | A_\mu^{(3)} | N(p, s) \rangle = 2m_N G^{(3)} s_\mu, \quad (2.2)$$

at vanishing momentum transfer.  $A_\mu^{(3)} = \frac{1}{2}(\bar{u}\gamma_\mu\gamma_5 u - \bar{d}\gamma_\mu\gamma_5 d)$  (here, notations  $u$  and  $d$  imply  $u$ -quark and  $d$ -quark fields respectively) and  $s_\mu = \bar{u}\gamma_\mu\gamma_5 u / (2m_N)$  is covariant spin-vector of the nucleon (here, notation  $u$  implies four-spinor, representing a spin-1/2 nucleon).

$$2m_N s_\mu \Delta\psi = \langle p, s | \bar{\psi}\gamma_\mu\gamma_5\psi | p, s \rangle. \quad (2.3)$$

$\Delta\psi(x)$  is a polarized PDF (Parton Distribution Function) [68],

$$\Delta\psi(x) = \psi^\uparrow(x) - \psi^\downarrow(x), \quad (2.4)$$

where  $\psi^\uparrow(x)(\psi^\downarrow(x))$  is the probability that the quark's spin is aligned (antialigned) with the nucleon spin at a given  $x$ .  $\Delta\psi = \int_0^1 dx \Delta\psi(x)$  is interpreted as the fraction of proton's spin which is carried by quarks (and antiquarks) of flavor  $\psi$ . In [17], the generalization of Goldberger-Treiman relation for  $\eta$  and  $\eta'$ , considering contributions from physical  $\eta$  and  $\eta'$  states only, has been done and values of  $g_{\eta NN}$  and  $g_{\eta' NN}$  were achieved. The Goldberger-Treiman relation for  $\eta$  and  $\eta'$  reads,

$$2m_N G_A^a = \sum_{P=\eta, \eta'} f_P^a g_{P NN}, a = 0, 8. \quad (2.5)$$

The flavor-singlet Goldberger-Treiman relation derived by Shore and Veneziano relates  $\eta^{(0)}$ -nucleon coupling constant to the flavor-singlet axial charge of the nucleon  $g_A^{(0)}$  extracted from polarized deep inelastic scattering [60, 69]. The relation in the chiral limit reads,

$$m_N g_A^{(0)} = \sqrt{\frac{3}{2}} F_0 (g_{\eta_0 NN} - g_{Q NN}), \quad (2.6)$$

Where  $g_{Q NN}$  is the effective gluonic coupling constant,  $F_0$  renormalizes the flavor-singlet decay constant. The large mass of  $\eta'$  and the small value of  $g_A^{(0)}$  indicates to substantial violation of OZI rule in the flavor singlet channel,  $J^P = 1^+$  [51]. By inserting phenomenological values of decay constants of  $\eta$  and  $\eta'$  mesons and using Eq. (2.5), the values of  $g_{\eta NN}$  and  $g_{\eta' NN}$  were estimated as  $3.4 \pm 0.5$  and  $1.4 \pm 1.1$  respectively in [17].

In [70], it was shown that the values obtained from direct generalization of GT relation for  $\pi^0$  to  $\eta, \eta'$ , differ largely from the values  $g_{\eta NN} = 6.8, g_{\eta' NN} = 7.3$  obtained by

potential model [71]. In [17], chiral symmetry breaking was not considered. In [70], the effect of chiral symmetry breaking was taken into account and with the use of dispersion relation, the values of  $g_{\eta NN}$  and  $g_{\eta' NN}$  were estimated as  $(4.95 - 5.45)$  and  $(5.6 - 10.9)$  respectively. These were in accord with those obtained from potential models.

Other approaches for calculating these coupling constants include chiral quark soliton model [72], fitting photoproduction data [66], potential model [73] and the QCD sum rules approach [36, 74, 75]. Basic features of QCD sum rules have been discussed in Chapter 1. To determine any hadronic parameter, following are the main steps in QCD Sum Rules technique:

1. Correlator is constructed by introducing interpolating field made out of fundamental quark and gluon fields carrying same quantum numbers as that of the hadron of interest.
2. Correlation function is calculated by Operator Product Expansion (OPE) at  $q^2 \rightarrow -\infty$  using QCD degrees of freedom.
3. Phenomenological form is constructed by using hadronic parameters.
4. Matching of the non-analytic part of the phenomenological form with the OPE calculation is carried to extract the hadronic parameter in terms of QCD parameters.

QCD sum rules have been used in past to calculate  $\eta$ -nucleon coupling constant  $g_{\eta NN}$  in SU(3) symmetry limit [74] as well as with SU(3)- flavor violating effects taken into account [76]; it has also been used to calculate singlet axial-vector coupling constant of the nucleon without resorting to any instanton contribution [77]. In Ref [76],  $\eta$  was considered as a member of octet family  $\eta_8$  and no mixing with the singlet  $\eta_0$  was taken into account for calculating  $g_{\eta NN}$ .

In the present work, we calculate the coupling constants of both physical  $\eta$  and  $\eta'$  mesons with a nucleon using quark-flavor basis which turns out to be more appropriate for working with a singlet component. Light-cone expansion of a quark

propagator naturally gives emission of anomalous gluons which couple to  $\eta$  and  $\eta'$  mesons. This is a characteristic contribution to  $g_{\eta NN}$  and  $g_{\eta' NN}$  having implication for nucleon spin problem [58].

## 2.2 Formalism and construction of Sum Rules

The content of this section and forthcoming sections is based on our work in [78]. General methods of calculating meson-nucleon coupling constants have been developed in Refs. [36, 74, 75, 79, 80]. Consider the correlator of the nucleon current between vacuum and one  $\eta^{(\prime)}$ -state,

$$\Pi(q, p) = i \int d^4x e^{iqx} \langle 0 | T \{ J_N(x), \overline{J}_N(0) \} | \eta^{(\prime)}(p) \rangle, \quad (2.7)$$

where  $J_N$  is the standard proton current [24].

$$J_N = \epsilon^{abc} [u^{aT} C \gamma_\mu u^b] \gamma_5 \gamma^\mu d^c, \quad (2.8)$$

Here a,b,c are color indices. The  $\eta^{(\prime)} NN$  coupling constant  $g_{\eta^{(\prime)} NN}$  is defined through the coefficient of the pole as[79]:

$$\overline{u}(qr)(\not{q} - M_n)\Pi(q, p)(\not{q} - \not{p} - M_n)u(ks) \big|_{q^2=M_n^2, (q-p)^2=M_n^2} = i\lambda^2 g_{\eta^{(\prime)} NN} \overline{u}(qr)\gamma_5 u(ks), \quad (2.9)$$

where  $k = q - p$ ,  $u(qr)$  is a Dirac spinor and  $\lambda$  is the coupling constant of the proton current with one-proton state [24].

$$\langle 0 | J_N(0) | q \rangle = \lambda u(q). \quad (2.10)$$

The correlator  $\Pi(x, p)$  in the coordinate space is written as [74],

$$\begin{aligned} \Pi(x, p) = & -i\epsilon_{abc}\epsilon_{a'b'c'} \{ \gamma_5 \gamma^\mu D_{cc'}^d \gamma^\nu \gamma_5 \{ Tr[iS_{aa'}(x)(\gamma_\nu C)^T iS_{bb'}^T(x)(C\gamma_\mu)^T] \\ & - Tr[iS_{ab'}(x)\gamma_\nu C iS_{ba'}^T(x)(C\gamma_\mu)^T] \} - \gamma_5 \gamma^\mu iS_{cc'} \gamma^\nu \gamma_5 \{ Tr[iS_{ab'}(x)\gamma_\nu C (D_{ba'}^u)^T (C\gamma_\mu)^T] \\ & - Tr[iS_{aa'}(x)(\gamma_\nu C)^T (D_{bb'}^u)^T (C\gamma_\mu)^T] - Tr[D_{aa'}^u (\gamma_\nu C)^T iS_{bb'}^T(x)(C\gamma_\mu)^T] \\ & + Tr[D_{ab'}^u \gamma_\nu C iS_{ba'}^T(x)(C\gamma_\mu)^T] \} \}. \end{aligned} \quad (2.11)$$

$D_{cc'}^q$  is defined as,

$$D_{cc'}^q = \frac{\delta_{cc'}}{12} A^q + \frac{\delta_{cc'}}{12} (\gamma^\mu \gamma_5) A_\mu^q - \frac{\delta_{cc'}}{12} (\gamma_5 \sigma^{\mu\nu}) A_{\mu\nu}^q. \quad (2.12)$$

For definitions of  $A^q$ ,  $A_\mu^q$  and  $A_{\mu\nu}^q$ , see Eq.(2.17). Following Ref. [79] we define the projected correlation function

$$\Pi_+(q, p) = \bar{u}(qr) \gamma_0 \Pi(q, p) \gamma_0 u(ks). \quad (2.13)$$

$\Pi_+$  can be regarded as a function of  $q_0$  in the reference frame in which  $\mathbf{q} = \mathbf{0}$ . The even and odd parts of the  $\Pi_+$  satisfy dispersion relations as,

$$\begin{aligned} \Pi_+^E(q_0^2) &= -\frac{1}{\pi} \int dq'_0 \frac{q'_0}{q_0^2 - q'^2_0} \text{Im} \Pi_+(q'_0), \\ \Pi_+^O(q_0^2) &= -\frac{1}{\pi} \int dq'_0 \frac{1}{q_0^2 - q'^2_0} \text{Im} \Pi_+(q'_0). \end{aligned} \quad (2.14)$$

On taking Borel transform [24, 79] with respect to  $q_0^2$  they take the form

$$\begin{aligned} \hat{B}[\Pi_+^E(q_0^2)] &= \frac{1}{\pi} \int dq'_0 q'_0 e^{\frac{-q'^2_0}{M^2}} \text{Im} \Pi_+(q'_0), \\ \hat{B}[\Pi_+^O(q_0^2)] &= \frac{1}{\pi} \int dq'_0 e^{\frac{-q'^2_0}{M^2}} \text{Im} \Pi_+(q'_0), \end{aligned} \quad (2.15)$$

where  $M$  is the Borel mass parameter. The RHS of Eq. (2.15) is expanded in terms of the observed spectral function. The absorptive part of the projected correlation function can be written as,

$$\begin{aligned} \text{Im} \Pi_+(q, p) &= -\bar{u}(qr) i \gamma_5 u(ks) \pi \lambda^2 g(q_0, \mathbf{p}^2) \left\{ \frac{\delta(q_0 - M_n)}{q_0 - E_k - \omega_p} + \frac{\delta(q_0 - E_k - \omega_p)}{q_0 - M_n} \right\} \\ &+ \left\{ \theta(q_0 - s_{\eta^{(\nu)}}) + \theta(-q_0 - s_{\eta^{(\nu)}}) \right\} \text{Im} \Pi_+^{OPE}(q, p), \end{aligned} \quad (2.16)$$

where  $s_{\eta^{(\nu)}}$  is the effective continuum threshold.

Mixing of decay constants and eigenstates are discussed in Chapter 1. For definitions of some important quantities  $f_M^{(q)}, f_M^{(s)}$  (see Eqs.(1.15-1.17)),  $h_M^{(q)}, h_M^{(s)}$  (see Eq.(3.14)). In QCD, the correlator is calculated via the operator product expansion

(OPE) at the deep space-like region  $q^2 \rightarrow -\infty$ . In the present approach, using vacuum saturation hypothesis, the quark-antiquark component with the  $\eta^{(\prime)}$  meson is factored out from the correlator. The rest of the correlator is time-ordered products of quark fields [74]. This is a light-cone expansion of the correlation function which is the first step in calculating Wilson coefficients of short-distance expansion (SDE). In the second step, SDE of light-cone operators is performed [79, 80]. Additionally, contribution to the correlator arising from radiatively generated anomalous gluons from quark propagators has also been taken into account. There are three kinds of nonlocal bilinear quark operators which contribute to the vacuum-to-meson matrix elements as given below. While the results on SDE of the matrix element of axial-vector type nonlocal quark operators have been taken from Ref. [74], the other two results, namely, those concerning pseudoscalar and tensor type nonlocal quark operators, have been calculated by us based on parametrization given in Refs. [81, 82]. Finally, quark-gluon mixed contribution to the matrix element are obtained by moving a gluon field-strength tensor from a quark propagator into the quark-antiquark component with a  $\eta^{(\prime)}$  meson. Our calculation of this matrix element is based on results and parametrization of Refs. [80, 82]. We list below the results of the vacuum-to- $\eta^{(\prime)}$  matrix elements of the light-cone operators used in this paper ( $q = u, d$ ):

$$A^q = \langle 0 | \bar{q}(0) i\gamma_5 q(x) | \eta^{(\prime)}(p) \rangle = \frac{h_q}{2\sqrt{2}m_q} \binom{C}{S} \left\{ 1 - \frac{ip \cdot x}{2} - \frac{(p \cdot x)^2}{6} + \frac{i(p \cdot x)^3}{24} \right\},$$

$$A_\mu^q = \langle 0 | \bar{q}(0) \gamma_\mu \gamma_5 q(x) | \eta^{(\prime)}(p) \rangle = \frac{f_q}{\sqrt{2}} \binom{C}{S} \left\{ 1 - \frac{ip \cdot x}{2} \right\} \left\{ ip_\mu - \frac{i\delta^2 p \cdot x x_\mu}{18} + \frac{5i\delta^2 x^2 p_\mu}{36} \right\},$$

$$A_{\mu\nu}^q = \langle 0 | \bar{q}(0) \gamma_5 \sigma^{\mu\nu} q(x) | \eta^{(\prime)}(p) \rangle = i \frac{h_q}{12\sqrt{2}m_q} \binom{C}{S} \left\{ p^\mu x^\nu - p^\nu x^\mu \right\} \\ \times \left\{ 1 - \frac{ip \cdot x}{2} - \frac{3(p \cdot x)^2}{20} + \frac{i(p \cdot x)^3}{30} \right\},$$

$$\langle 0 | q^a(x) g G_{\mu\nu}^n \left(\frac{x}{2}\right) \bar{q}^b(0) | \eta^{(\prime)}(p) \rangle = i \binom{C}{S} \frac{(t^n)_{ab}}{16\sqrt{2}} \left\{ f_q \gamma_5 a_1 (p_\nu \gamma_\mu - p_\mu \gamma_\nu) p \cdot x + \right.$$



$$\begin{aligned}
& a_2 \not{p}(p_\mu x_\nu - p_\nu x_\mu) - f_{3\pi} \gamma_5 p^\alpha (p_\mu \sigma_{\alpha\nu} - p_\nu \sigma_{\alpha\mu}) (1 - \frac{ip \cdot x}{2}) \\
& - f_q \epsilon_{\mu\nu\alpha\beta} \gamma^\alpha p^\beta \frac{\delta^2}{3} (1 - \frac{ip \cdot x}{2}) \Big\}, \tag{2.17}
\end{aligned}$$

where  $\begin{pmatrix} C \\ S \end{pmatrix} = \begin{pmatrix} \cos \phi \\ \sin \phi \end{pmatrix}$ ,  $a_1 = \begin{pmatrix} 0.0074 \\ 0.0062 \end{pmatrix}$ ,  $a_2 = \begin{pmatrix} 0.0136 \\ 0.0149 \end{pmatrix}$  for  $\begin{pmatrix} \eta \\ \eta' \end{pmatrix}$ ,  $\phi$  is mixing angle in quark-flavor scheme [17]. The relevant gluonic term can be extracted from the light-cone expansion of the quark propagator [83]:

$$\begin{aligned}
\langle 0 | T\{q(x)\bar{q}(0)\} | 0 \rangle &= \frac{\Gamma(-\epsilon)}{32\pi^2(-x^2)^{-\epsilon}} x^\mu \gamma^\lambda \gamma_5 g^2 \int_0^1 du \int_0^u dv [(1 - 2\bar{u} \\
&\quad - 2v) G_{\mu\nu}(ux) \tilde{G}^\nu{}_\lambda(vx) - \tilde{G}_{\mu\nu}(ux) G^\nu{}_\lambda(vx)] + \dots \\
&\rightarrow \frac{\Gamma(-\epsilon)}{32\pi^2(-x^2)^{-\epsilon}} g^2 x^\mu \gamma^\lambda \gamma_5 t^a t^b G_\mu^{a\nu}(0) G_{\nu\lambda}^b(0) \int_0^1 du \int_0^u dv (-2\bar{u} \\
&\quad - 2v) + \dots \\
&\rightarrow \frac{\Gamma(-\epsilon)\alpha_s}{72 \times 4\pi(-x^2)^{-\epsilon}} G\tilde{G} \not{x} \gamma_5 + \dots \tag{2.18}
\end{aligned}$$

for dimension  $d=4-2\epsilon$ ,  $G\tilde{G}$  is evaluated at the origin in the spirit of short distance expansion and ellipsis stand for other structures. Here  $G\tilde{G} = \frac{1}{2}\epsilon^{\mu\nu\rho\sigma} G_{\mu\nu}^a G_{\rho\sigma}^a$ ,  $\epsilon^{0123} = +1$ . Defining matrix element [84],

$$\langle 0 | \frac{\alpha_s}{4\pi} G\tilde{G} | \eta^{(\prime)}(p) \rangle = a_{\eta^{(\prime)}}, \tag{2.19}$$

we can write:

$$\langle 0 | T\{q(x)\bar{q}(0)\} | \eta^{(\prime)} \rangle = \frac{\Gamma(-\epsilon)}{72} (-x^2)^\epsilon a_{\eta^{(\prime)}} \not{x} \gamma_5 + \dots \tag{2.20}$$

where

$$\begin{aligned}
a_\eta &= -\frac{m_{\eta'}^2 - m_\eta^2}{\sqrt{2}} \sin \phi \cos \phi (-f_q \sin \phi + \sqrt{2} f_s \cos \phi), \\
a_{\eta'} &= -\frac{m_{\eta'}^2 - m_\eta^2}{\sqrt{2}} \sin \phi \cos \phi (f_q \cos \phi + \sqrt{2} f_s \sin \phi). \tag{2.21}
\end{aligned}$$

The removal of divergence requires renormalization and we do this in  $\overline{\text{MS}}$  scheme. In  $\Pi(q, p)$  the operator  $G\tilde{G}$  originates from only d-quark line and there is no contribution where gluons originate from two different quark lines.

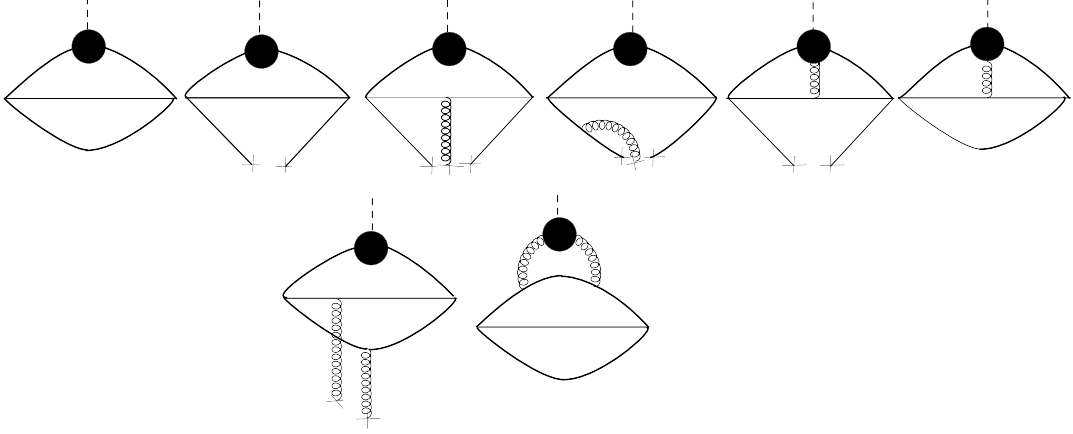


Figure 2.1: Feynman diagrams considered for the correlation function  $\Pi(q, p)$ . The dotted line stands for the meson.

We get the following result for the correlator:

$$\begin{aligned}
\Pi(q, p) &= \frac{f_q}{\sqrt{2}} \left( \begin{matrix} C \\ S \end{matrix} \right) \left\{ \frac{i}{6\pi^2} \left[ \not{p} \left( \log(-q^2) \left\{ q^2 - 2q \cdot p - \delta^2 \right\} + \frac{\delta^2 2q \cdot p}{q^2} - 3 \log(-q^2) \right. \right. \right. \\
&\quad \left. \left. \left\{ q^2 - q \cdot p - \delta^2 \right\} - \frac{8\delta^2 q \cdot p}{3q^2} \right) + \not{q} \left( \log(-q^2) \left\{ 2q \cdot p - p^2 \right\} - \frac{2(q \cdot p)^2}{q^2} \right. \right. \\
&\quad \left. \left. + \delta^2 \left\{ \frac{p^2}{q^2} - \frac{2(p \cdot q)^2}{q^4} \right\} - \frac{\delta^2 2q \cdot p}{q^2} - \frac{2\delta^2}{3} \left\{ \frac{q \cdot p}{q^2} - \frac{p^2}{2q^2} + \frac{(q \cdot p)^2}{q^4} \right\} \right) \right] \gamma_5 \\
&\quad + \frac{i \langle g^2 G^2 \rangle}{144\pi^2} \left[ \not{p} \left( -\frac{4}{q^2} - \frac{3q \cdot p}{q^4} + \frac{8\delta^2}{9q^4} \right) + \not{q} \left( \frac{p^2 - 2q \cdot p}{q^4} - \frac{4(q \cdot p)^2}{q^6} - \frac{32\delta^2 q \cdot p}{9q^6} \right) \right] \gamma_5 \\
&\quad - \frac{i\delta^2}{18\pi^2} \left[ \not{p} \log(-q^2) + \frac{2\not{q} q \cdot p}{q^2} - \frac{\not{q} p^2}{q^2} - \frac{\not{p} q \cdot p}{q^2} + \frac{2\not{q} (q \cdot p)^2}{q^4} \right] \gamma_5 \Big\} \\
&\quad - \frac{i\not{q} \gamma_5 a_{\eta^{(\prime)}} \log\left(\frac{-q^2}{\mu^2}\right)}{6\pi^2} \left\{ 3 + \log(4) - 2\gamma - \frac{1}{2} \log\left(\frac{-q^2}{\mu^2}\right) \right\} + \frac{ih_q \langle \bar{q} q \rangle}{18\sqrt{2}m_q} \left( \begin{matrix} C \\ S \end{matrix} \right) \times \\
&\quad \left\{ \frac{2\not{p}}{q^2} + \frac{1}{q^4} \left[ 4\not{q} p \cdot q - 2\not{q} p^2 + \frac{8\not{q} (q \cdot p)^2}{q^2} - \frac{3}{5} \left( -\not{p} p^2 + \frac{12}{q^2} \left\{ \not{q} p^2 p \cdot q + \frac{\not{p} (p \cdot q)^2}{3} \right. \right. \right. \right. \\
&\quad \left. \left. \left. - \frac{2\not{q} (p \cdot q)^3}{q^4} \right\} \right) \right] \right\} \gamma_5 - \frac{ih_q \langle \bar{q} g \sigma \cdot G q \rangle}{24\sqrt{2}m_q q^4} \times \left( \begin{matrix} C \\ S \end{matrix} \right) \left\{ \not{p} - \frac{4\not{q} q \cdot p}{q^2} \right\} \gamma_5 + \frac{h_q i \gamma_5}{8\pi^2 \sqrt{2} m_q} \\
&\quad \times \left( \begin{matrix} C \\ S \end{matrix} \right) \left\{ \log(-q^2) (q^2 - q \cdot p) + \frac{1}{3} \left[ p^2 \log(-q^2) + \frac{2(q \cdot p)^2}{q^2} \right] - \right. \\
&\quad \left. \frac{1}{3} \left[ \frac{3p^2 p \cdot q}{2q^2} - \frac{(p \cdot q)^3}{q^4} \right] \right\} - \langle g^2 G^2 \rangle \frac{i\gamma_5 h_q}{192\pi^2 \sqrt{2} m_q} \left( \begin{matrix} C \\ S \end{matrix} \right) \left\{ \frac{1}{q^2} + \frac{p \cdot q}{q^4} - \frac{1}{3} \left[ \frac{p^2}{q^4} - \frac{4(p \cdot q)^2}{q^6} \right] \right\} + \\
&\quad \frac{i\gamma_5 f_{3\pi}}{4\pi^2 \sqrt{2}} \left( \begin{matrix} C \\ S \end{matrix} \right) \times \left\{ p^2 \log(-q^2) + \frac{2(q \cdot p)^2}{q^2} - 4p^2 \log(-q^2) - \frac{3p^2 (q \cdot p)}{q^2} + \frac{2(q \cdot p)^3}{q^4} + \right. \\
&\quad \left. \frac{4p^2 (q \cdot p)}{q^2} \right\} + \sigma^{\alpha\beta} p_{\alpha} q_{\beta} \gamma_5 \times \left\{ \frac{h_q}{12\sqrt{2}\pi^2 m_q} \left( \begin{matrix} C \\ S \end{matrix} \right) \times \left[ -\frac{\log(-q^2)}{4} + \frac{(p \cdot q)}{4q^2} - \right. \right. \\
&\quad \left. \left. \frac{3}{10} \left( \frac{p^2}{q^2} - \frac{2(p \cdot q)^2}{q^4} \right) + \frac{1}{30} \left( \frac{4(q \cdot p)^3}{q^6} - \frac{3p^2 q \cdot p}{q^4} \right) + \frac{\langle g^2 G^2 \rangle}{288q^4} \left( 1 + \frac{2q \cdot p}{q^2} \right) \right] - \langle \bar{q} q \rangle \frac{2f_q}{3\sqrt{2}} \times \right.
\end{aligned}$$

$$\begin{aligned} & \binom{C}{S} \left[ \frac{2}{q^2} + \frac{2q \cdot p}{q^4} + \frac{10\delta^2}{9q^4} + \frac{20\delta^2 p \cdot q}{9q^6} \right] + \frac{2f_q \delta^2 \langle \bar{q}q \rangle}{9\sqrt{2}q^4} \binom{C}{S} \times \left[ 1 + \frac{2p \cdot q}{q^2} \right] \\ & - \frac{\langle \bar{q}g\sigma \cdot Gq \rangle f_q}{4\sqrt{2}q^4} \binom{C}{S} \left[ 1 + \frac{2q \cdot p}{q^2} \right] \}. \end{aligned} \quad (2.22)$$

From Eqs. (2.15) and (2.16), we get

$$\begin{aligned} \frac{1}{\pi} \int dq'_0 e^{(-\frac{q_0'^2}{M^2})} \hat{B} \text{Im} \Pi_+(q', p) &= \bar{u}(q) i\gamma_5 u(q-p) \frac{\lambda^2}{E_k + \omega_p - M_n} \left\{ e^{-\frac{M_n^2}{M^2}} g(M_n, \mathbf{p}^2) \right. \\ &\quad \left. - e^{-\frac{(E_k + \omega_p)^2}{M^2}} g(E_k + \omega_p, \mathbf{p}^2) + \text{cont.} \right\}, \\ \frac{1}{\pi} \int dq'_0 dq'_0 e^{(-\frac{q_0'^2}{M^2})} \hat{B} \text{Im} \Pi_+(q', p) &= \bar{u}(q) i\gamma_5 u(q-p) \frac{\lambda^2}{E_k + \omega_p - M_n} \left\{ e^{-\frac{M_n^2}{M^2}} g(M_n, \mathbf{p}^2) M_n - \right. \\ &\quad \left. e^{-\frac{(E_k + \omega_p)^2}{M^2}} (E_k + \omega_p) g(E_k + \omega_p, \mathbf{p}^2) + \text{cont.} \right\}, \end{aligned} \quad (2.23)$$

where last terms stand for the continuum contributions. Similarly, we can get Borel transform of OPE expression  $\Pi(q, p)_{\text{even}}^{\text{OPE}}$  and  $\Pi(q, p)_{\text{odd}}^{\text{OPE}}$ . In the region of  $M^2$  where sum rules work, we can equate the coefficients of  $\bar{u}(q) i\gamma_5 u(q-p)$  in the phenomenological expression Eq. (2.23) to the coefficients of the same in OPE expressions and transfer the continuum contribution to the OPE side. The coefficient of  $\bar{u}(q) i\gamma_5 u(q-p)$  in the OPE expression for  $\Pi_{+odd}$  gives:

$$\begin{aligned} \hat{B} [\Pi_{+odd}^{\text{OPE-cont.}}] &= M^2 \left\{ \frac{f_q \mathbf{p}^2}{3\sqrt{2}\pi^2} \binom{C}{S} - \frac{a_{\eta^{(\prime)}}}{6\pi^2} [3 + \ln 4 - 3\gamma + \ln M^2] + \frac{h_q}{8\sqrt{2}\pi^2 m_q} \binom{C}{S} \times \right. \\ &\quad \left[ \frac{5}{6} M_n - \frac{7}{6} E_k \right] \Big\} E_0 \left( \frac{s_{\eta^{(\prime)}}}{M^2} \right) + \frac{h_q}{8\sqrt{2}\pi^2 m_q} \binom{C}{S} \left\{ \frac{1}{3} (M_n - E_k)^2 [2M_n + E_k] + \right. \\ &\quad \left. \frac{2}{5} E_k \mathbf{p}^2 \right\} - \frac{f_{3\pi}}{4\sqrt{2}\pi^2} \binom{C}{S} 2(M_n - E_k)^2 \left\{ 2M_n - E_k \right\} - \frac{4}{3\sqrt{2}} f_q \binom{C}{S} \langle \bar{q}q \rangle \times \\ &\quad \left\{ M_n + E_k \right\} + \frac{f_q \delta^2}{6\sqrt{2}\pi^2} \binom{C}{S} \left\{ M_n - E_k \right\} \frac{4}{3} E_k + \frac{1}{M^2} \left\{ \frac{1}{18\sqrt{2}} f_q \binom{C}{S} \times \right. \\ &\quad \left. \langle \frac{\alpha_s}{\pi} G^2 \rangle [M_n - E_k] [M_n - 5E_k] + \frac{h_q \langle \bar{q}q \rangle}{9\sqrt{2}m_q} \binom{C}{S} [M_n - E_k] [4E_k - 2M_n] \right. \\ &\quad \left. - \frac{h_q \langle \frac{\alpha_s}{\pi} G^2 \rangle}{48 \times 18\sqrt{2}m_q} \binom{C}{S} [19M_n - 17E_k] + \frac{f_q}{\sqrt{2}} \binom{C}{S} [M_n + E_k] \left[ \frac{14}{27} \langle \bar{q}q \rangle \delta^2 \right. \right. \\ &\quad \left. \left. + \frac{1}{4} \langle \bar{q}g\sigma \cdot Gq \rangle \right] \right\}, \end{aligned} \quad (2.24)$$

where  $E_k = \sqrt{M_n^2 + \mathbf{p}^2}$ ,  $\omega_p = \sqrt{m_{\eta^{(\prime)}}^2 + \mathbf{p}^2}$ . The continuum contribution has been parameterized in a standard way [24] through  $E_0(x) = 1 - e^{-x}$ . Unlike the case of  $g_{\pi NN}$ , here we have retained terms up to  $O((M_n - E_k)^3)$ . We have numerically

checked that the short-distance expansion, as given in Eq.(2.17), works. We also use nucleon mass sum rule [24]:

$$M_n \lambda^2 e^{-M_n^2/M^2} = \frac{1}{4\pi^2} \left\{ -M^4 \langle \bar{q}q \rangle E_1\left(\frac{s_0}{M^2}\right) + \frac{\pi^2}{6} \langle \bar{q}q \rangle \left\langle \frac{\alpha_s}{\pi} G^2 \right\rangle \right\} \equiv \hat{B}[\Pi^m]. \quad (2.25)$$

At the physical point, where both the nucleon lines and the meson line are on mass-shell with  $\mathbf{p}^2 = -m_{\eta^{(\prime)}}^2 + \frac{m_{\eta^{(\prime)}}^4}{4M_n^2}$ , RHS of Eq. (2.15), combined with Eq. (2.16), takes  $\frac{0}{0}$  form and hence cannot be used to determine the coupling constants directly in this approach. However, we can determine  $g_{\eta^{(\prime)}NN}$  at different kinematical points and extrapolate the results to the physical point. Working with  $\Pi_{+odd}$ , from the ratio of the two sum rules the coupling constant can be obtained as:

$$\frac{g(M_n, \mathbf{p}^2)}{M_n(E_k + \omega_p - M_n)} = \frac{\hat{B}[\Pi_{+odd}^{OPE-cont.}]}{\hat{B}[\Pi^m]} - \frac{M^4}{(E_k + \omega_p)^2 - M_n^2} \frac{d}{dM^2} \left( \frac{\hat{B}[\Pi_{+odd}^{OPE-cont.}]}{\hat{B}[\Pi^m]} \right). \quad (2.26)$$

Following values of parameters have been used for estimation of  $g_{\eta^{(\prime)}NN}$  (all quantities are in GeV unit) [24, 74, 76, 77, 79]:  $\langle \bar{q}q \rangle = -(1.65 \pm 0.15) \times 10^{-2}$ ,  $\langle \frac{\alpha_s}{\pi} G^2 \rangle = 0.005 \pm 0.004$ ,  $\delta^2 = 0.2 \pm 0.04$ ,  $f_q = (1.07 \pm 0.02)f_\pi$ ,  $f_s = (1.34 \pm 0.06)f_\pi$ ,  $s_{\eta^{(\prime)}} = 2.57 \pm 0.03$ ,  $s_0 = 2.5$ ,  $f_{3\pi} = 0.0045$ ,  $\phi = 40^\circ \pm 1^\circ$ ,  $\frac{h_q}{m_q} = -4 \frac{f_q}{f_\pi^2} \langle \bar{q}q \rangle$  [85],  $\langle \bar{q}g\sigma \cdot Gq \rangle = m_0^2 \langle \bar{q}q \rangle$ ,  $m_0^2 = 0.8 \pm 0.1$ .

## 2.3 Analysis of sum Rules and results

We have plotted the coupling constant  $g$  obtained from Eq. (2.26) in Figs. (2.2) and (2.3) as a function of  $M^2$  for different values of  $\mathbf{p}^2$ . Our chosen range of the Borel mass is  $0.8 \text{ GeV}^2 < M^2 < 1.8 \text{ GeV}^2$  for  $\eta'$  and  $1.5 \text{ GeV}^2 < M^2 < 2.5 \text{ GeV}^2$  for  $\eta$ . This is done with an eye to keep continuum contribution and contribution of  $1/M^2$  terms less than 30 % and to keep  $g_{\eta^{(\prime)}NN}$  not too low. A similar analysis with the even correlation function  $\Pi_+^E$  gives a large continuum contribution and the large contribution of  $1/M^2$  terms, hence the result is not reliable. In Table. 2.1, we have displayed our results for coupling constants, coupling constants without gluonic contribution, the gluonic contribution to the coupling constants and the

contribution coming from the OZI-rule violating s-quark ( $f_s$  term in  $a_{\eta^{(\prime)}}$ , see Eq. (2.21)). It is clear from the Table that though the gluonic contribution and the OZI rule violating contribution from s-quark are small at the physical point, they become significantly large off the physical point and eventually become dominant at far off physical point for  $\eta'$ . These coupling constants off the physical point will be important for some processes such as the photo-production of mesons off a nucleon target. We have made error estimates of our results as follows: Errors due to different phenomenological parameters, as given above, and error due to finite slope and finite range of the Borel mass have been shown separately. Error due to deviation from linear extrapolation is small and is neglected.

$$\begin{aligned} g_{\eta NN} &= 0.96^{+0.16}_{-0.17}(M^2)^{+0.14}_{-0.15}(\text{rest}), \\ g_{\eta' NN} &= 0.76^{+0.27}_{-0.08}(M^2)^{+0.24}_{-0.24}(\text{rest}). \end{aligned} \quad (2.27)$$

The flavor-singlet Goldberger-Treiman relation for QCD was derived by Shore and Veneziano [69](written in our notation),

$$M_n g_A^{(0)} = \sqrt{\frac{3}{2}} [f^{0\eta'} (g_{\eta' NN} + g_{gluon}^{(\eta')}) + f^{0\eta} (g_{\eta NN} + g_{gluon}^{(\eta)})] \quad (2.28)$$

Using our results for  $g_{\eta^{(\prime)} NN}$  and  $g_{gluon}^{(\eta^{(\prime)})}$ , and  $f^{0\eta^{(\prime)}}$  from Ref. [60], we get  $g_A^{(0)} = (0.23 - 0.28)$  in the range of medium to maximum values of the parameters. The comparison of our estimation of  $g_A^0$  with literature is given in Table. 2.2.

Table 2.1: Values of  $g_{\eta NN}$  and  $g_{\eta' NN}$  obtained at different non-physical points and extrapolated to the physical point. Values of coupling constants due to gluonic operator  $\alpha_s G\tilde{G}$ , contribution without gluonic operator and s-quark contribution as it appears in  $a_{\eta^{(\prime)}}$  are also shown.

	$g_{\eta NN} (M^2=2\text{GeV}^2)$			$g_{\eta' NN} (M^2=1.3\text{GeV}^2)$			
$\mathbf{p}^2$	$-m_\eta^2/2$	$-\frac{3}{4}m_\eta^2$	$-m_\eta^2 + \frac{m_\eta^4}{4M_n^2}$	$-m_{\eta'}^2/2$	$-2\frac{m_{\eta'}^2}{3}$	$-\frac{3}{4}m_{\eta'}^2$	$-m_{\eta'}^2 + \frac{m_{\eta'}^4}{4M_n^2}$
$g_{\text{total}}$	1.88	1.32	0.96	3.07	1.69	0.94	1.03
$g_{\text{no-gluon}}$	1.45	1.26	1.13	1.22	1.31	1.44	1.42
$g_{\text{gluon}}$	0.43	0.06	-0.17	1.85	0.38	-0.50	-0.39
$g_s$	0.82	0.12	-0.34	1.11	0.23	-0.3	-0.24

Table 2.2: Comparison of  $g_A^{(0)}$  estimated by us with the literature.

Reference	$g_A^0$
This Work(QCDSR+GT relation)	0.23-0.28
COMPASS ( $Q^2 = 3GeV^2$ ) [86]	0.26-0.36
NNPDFPoll.1( $Q^2 = 10GeV^2$ ) [87]	$0.25 \pm 0.10$
Theory [77]	$0.39 \pm 0.05 \pm 0.04$
Lattice QCD [88]	0.405

Table 2.3: Comparison of our results on  $g_{\eta NN}$  and  $g_{\eta' NN}$  with results for the same from recent literature.

Ref.	$g_{\eta NN}$	$g_{\eta' NN}$	Comment
Present work	(0.64 – 1.26)	(0.44 – 1.27)	QCD sum rule
[70]	(4.95 – 5.45)	(5.6 – 10.9)	GT relation+ Dispersion relation
[17]	(3.4 ± 0.5)	(1.4 ± 1.1)	Theory (GT relation)
[65]	2.241	–	Photoproduction
[60]	(3.78 ± 0.34)	(1 – 2)	Theory
[64]	(0.39, 0.92)	–	Photoproduction+(Isobar model, Dispersion relation)
[66]	0.89	0.87	Fitting photoproduction data
[76]	4.2 ± 1.05	–	QCDSR at unphysical point
[72]	4.399 ± 0.365	2.166 ± 0.312	Chiral quark-soliton model
[73]	6.852	8.66	Potential model

## 2.4 Summary and conclusion

We have used QCD sum rules, a well-tested approach in hadron physics, to calculate  $g_{\eta NN}$  and  $g_{\eta' NN}$ . The flavor-singlet contribution has been facilitated by use of quark-flavor basis. A characteristic contribution from radiatively generated gluonic operator  $\alpha_s G\tilde{G}$  was explicitly included. Finally, the values of the coupling constants at the physical point were estimated from linear extrapolation of results obtained at two other points. Anomalous glue, which gives excess mass to the would-be Goldstone bosons  $\eta$  and  $\eta'$  on the one end and a fraction of spin to the nucleon on the other end, also gives substantial contribution to the coupling constants of these mesons to the nucleon. Radiatively generated gluons, which eventually go to the mesons, are attached to the valance d-quark for the proton and to the valance  $u$ -quark for the neutron. Though interpolating fields of nucleons consist of  $u$ - and  $d$ -quark fields only, the coupling constants of the nucleon with  $\eta$  and  $\eta'$  contain a term proportional to  $f_s$ . This can be considered as OZI-violating contribution to

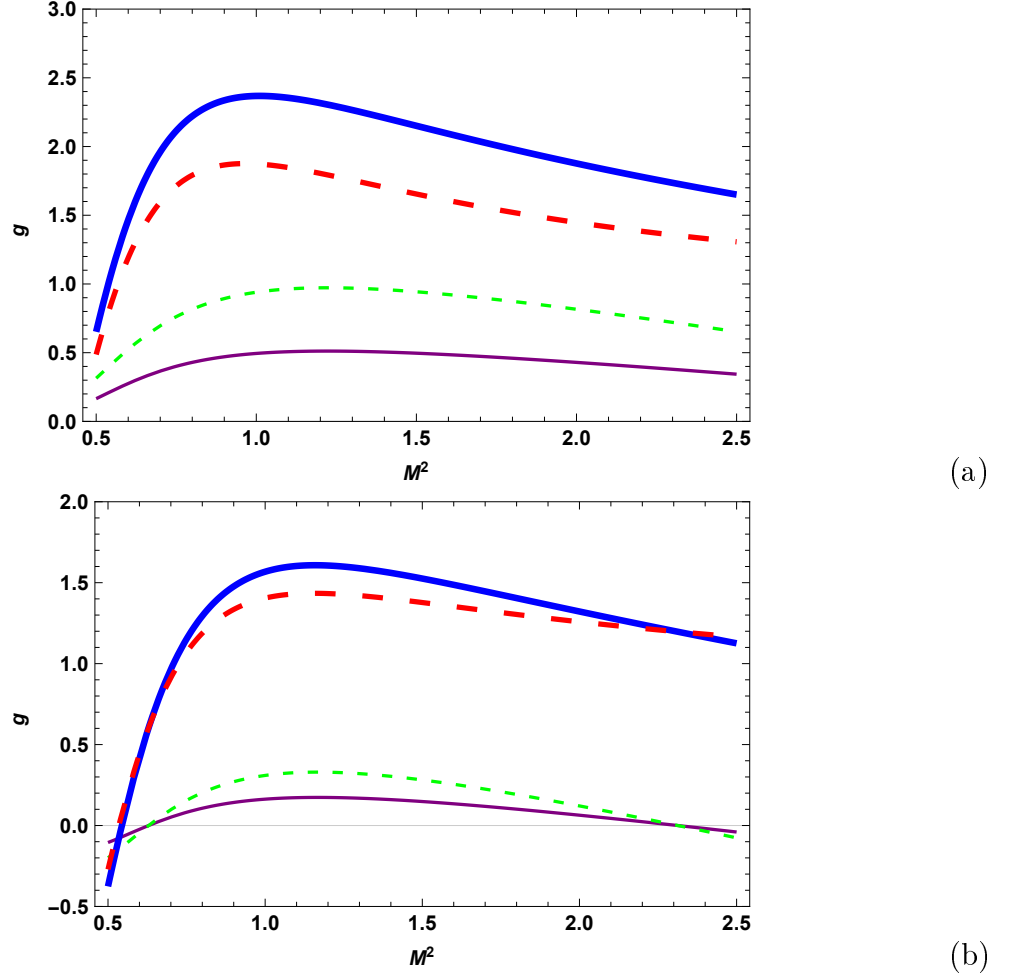
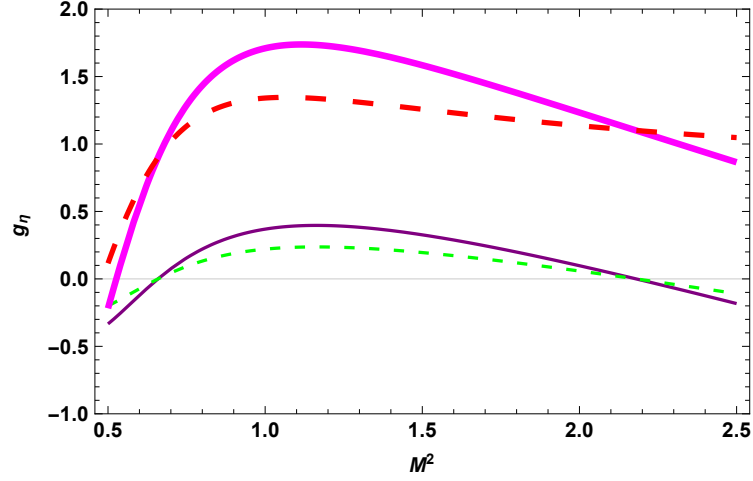
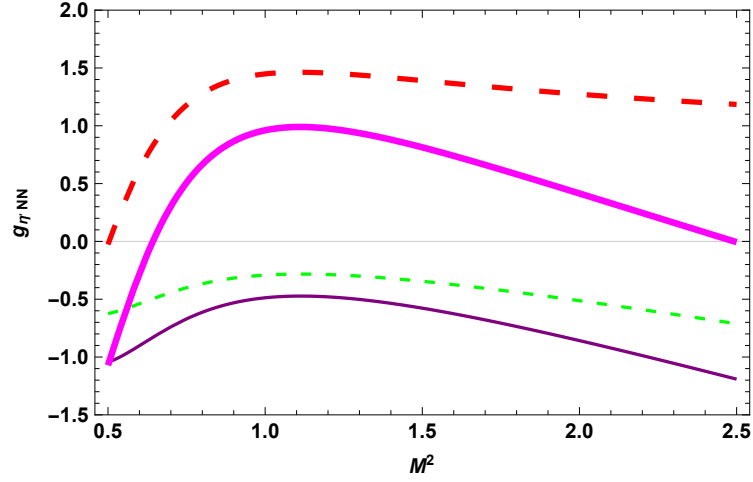


Figure 2.2: Plots of our results for  $g_{\eta NN}$  as a function of  $M^2$  (thick solid line). Also plotted are our results on  $g_{\eta NN}$  without contribution from gluonic operator  $\alpha_s G\tilde{G}$  (long-dashed line), only due to  $\alpha_s G\tilde{G}$  (thin solid line) and due to the part with  $f_s$  in  $a_\eta$  (short-dashed line). Figs.(a) and (b) are for  $\eta$  when  $\mathbf{p}^2$  is  $-\frac{m_\eta^2}{2}$  and  $-\frac{3m_\eta^2}{4}$  respectively.

the meson-nucleon coupling constant and is substantial for both  $\eta$  and  $\eta'$  mesons. Though  $\eta$  is largely octet, the gluon contribution to the  $g_{\eta NN}$  turns out to be significant. The branching ratios for  $N^*(1535)$  to decay to  $\eta N$  and  $\pi N$  final states are approximately equal, about 45%, even though the latter channel has larger phase space. The result is interpreted as evidence for a possible gluon anomaly contribution to the decay by Olbrich et al. [89]. Understanding of non-perturbative gluon dynamics and axial  $U(1)$  anomaly has a vital role in future development of hadron physics and nuclear physics and our results on  $g_{\eta NN}$  and  $g_{\eta' NN}$  will be useful for this.



(a)



(b)

Figure 2.3: Plots of our results for  $g_{\eta' NN}$  as a function of  $M^2$  (thick solid line). Also plotted are our results on  $g_{\eta' NN}$  without contribution from gluonic operator  $\alpha_s G\tilde{G}$  (long-dashed line), only due to  $\alpha_s G\tilde{G}$  (thin solid line) and due to the part with  $f_s$  in  $a_{\eta'}$  (short-dashed line). Figs.(a) and (b) are for  $\eta'$  when  $\mathbf{p}^2$  is  $-\frac{2m_{\eta'}^2}{3}$  and  $-\frac{3m_{\eta'}^2}{4}$  respectively.

## 2.5 Appendix

Here, we give few important steps for calculation of correlation function for one of the OPE diagrams given in Fig. (2.1). In order to show the steps, let us consider diagram shown in Fig. (2.4). We use expressions (2.11, 2.12) and (2.17).



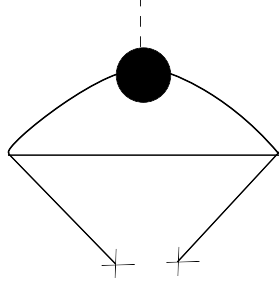


Figure 2.4: A Feynman diagram with a quark condensate contributing to the correlation function  $\Pi(x, p)$ .

The quark Green's function is expanded as [90],

$$\begin{aligned} \langle 0 | T \{ \psi_i^a(x) \bar{\psi}_k^b(0) \} | 0 \rangle = & \delta^{ab} \left[ \frac{i}{2\pi^2 x^4} \not{x}_{ik} - \frac{m_\psi \delta_{ik}}{4\pi^2 x^2} - \delta_{ik} \frac{\langle \bar{\psi} \psi \rangle}{12} + \frac{i m_\psi \langle \bar{\psi} \psi \rangle}{48} \not{x}_{ik} \right. \\ & \left. - \delta_{ik} \frac{x^2}{192} \langle \bar{\psi} g_s \sigma \cdot G \psi \rangle + \not{x}_{ik} \frac{i x^2}{3^2 2^7} m_\psi \langle \bar{\psi} g_s \sigma \cdot G \psi \rangle - \left[ \frac{\lambda^n}{2} \right]^{ab} (\not{x} \sigma^{\alpha\beta} + \sigma^{\alpha\beta} \not{x})_{ik} \frac{i}{32\pi^2 x^2} g_s G_{\alpha\beta}^n + \dots \right] \end{aligned} \quad (2.29)$$

Using Eqs. (2.12), (2.29) in Eq. (2.11),

$$\begin{aligned} \Pi(x, p) = & i \epsilon_{abc} \epsilon_{a'b'c'} \gamma_5 \gamma^\mu \delta_{cc'} i \frac{\not{x}}{2\pi^2 x^4} \gamma^\nu \gamma_5 \\ & Tr [C \gamma_\mu \frac{\delta_{ba'}}{12} [(\gamma^\sigma \gamma_5) A_\sigma^q + i \gamma_5 A^q - \frac{1}{2} \sigma^{\sigma\delta} A_{\sigma\delta}^q] \gamma_\nu C (\frac{-\delta_{ab'} \langle \bar{q} q \rangle}{12})], \end{aligned} \quad (2.30)$$

Above equation, after a few simplifications, reduces to,

$$\Pi(x, p) = -4 * 2i \frac{\langle \bar{q} q \rangle \gamma_5}{\pi^2 x^4 12} [x^\sigma \gamma^\delta - x^\delta \gamma^\sigma] A_{\sigma\delta}^q. \quad (2.31)$$

Factor of 4 in above equation appears due to contribution of all terms in the Eq. (2.11). Using expansion for  $A_{\sigma\delta}^q$  (see Eq. (2.17)),

$$\begin{aligned} \Pi(x, p) = & -8i \frac{\langle \bar{q} q \rangle \gamma_5}{\pi^2 x^4 12} [x^\sigma \gamma^\delta - x^\delta \gamma^\sigma] \times \\ & i \frac{h_q}{12\sqrt{2}m_q} \binom{C}{S} \left\{ p_\sigma x_\delta - p_\delta x_\sigma \right\} \left\{ 1 - \frac{ip \cdot x}{2} - \frac{3(p \cdot x)^2}{20} + \frac{i(p \cdot x)^3}{30} \right\}, \end{aligned} \quad (2.32)$$

For the purpose of fourier transform, we use following formulas [91].

$$\begin{aligned}
\int e^{iqx} \frac{1}{x^2} &= -\frac{4i\pi^2}{q^2}, \\
\int e^{iqx} \frac{x_\alpha x_\beta}{x^4} &= -2i\pi^2 \left[ \frac{g_{\alpha\beta}}{q^2} - \frac{2q_\alpha q_\beta}{q^4} \right], \\
\int e^{iqx} \frac{x_\alpha x_\beta x_\rho}{x^4} &= 4\pi^2 \left[ \frac{1}{q^4} \{q_\alpha g_{\rho\beta} + q_\beta g_{\rho\alpha} + q_\rho g_{\alpha\beta}\} - \frac{4q_\alpha q_\beta q_\rho}{q^6} \right], \\
\int e^{iqx} \frac{x_\alpha x_\beta x_\rho x_\delta}{x^4} &= -4i\pi^2 \left[ \frac{1}{q^4} \{g_{\alpha\delta} g_{\rho\beta} + g_{\beta\delta} g_{\rho\alpha} + g_{\rho\delta} g_{\alpha\beta}\} - \frac{4}{q^6} \{q_\alpha q_\delta g_{\rho\beta} + q_\beta q_\delta g_{\rho\alpha} \right. \\
&\quad \left. + q_\rho q_\delta g_{\alpha\beta} + q_\alpha q_\rho g_{\beta\delta} + q_\beta q_\rho g_{\alpha\delta} + q_\alpha q_\beta g_{\rho\delta}\} \right], \tag{2.33}
\end{aligned}$$

Upon Fourier transform, Eq. (2.32) reduces to,

$$\Pi(q, p) = -4i \langle \bar{q} q \rangle \gamma_5 \frac{ih_q}{3\pi^2 12\sqrt{2}m_q} \left[ 12 \frac{\not{p}}{q^2} + \frac{1}{q^4} \left( (2p^2 - 32p \cdot q) \not{q} + (8p \cdot q - 3p^2) \not{p} \right) + \mathcal{O}(1/q^6) \right]. \tag{2.34}$$

Above result shows the contribution of Fig. (2.4) to the total OPE result in the momentum space. Other diagrams have been calculated in a similar manner and Borel transformation have been performed as a next step.